Ibn Al-Haitham Journal for Pure and Applied Sciences
Journal homepage: jih.uobaghdad.edu.iq
PISSN: 1609-4042, EISSN: 2521-3407
IHJPAS. 2024, 37(4)

Theoretical Study of Energy Loss of Proton in Human Tissues

***Musaab I. Mohammed**
General Directorate of Education of Salah Uddin, Salah Uddin, Iraq.
*Corresponding Author

Received: 28 June 2023 Accepted: 1 August 2023 Published: 20 October 2024
doi.org/10.30526/37.4.3636

Abstract

In this paper, a theoretical study was carried out to calculate the proton energy loss in human tissues (Adipose tissue, Blood, Bone (Compact), Bone (Cortical), Brain, Eye lens, Lung, Skin, and Testicles) within the energy range of 1 MeV to 1000 MeV. We calculated the total stopping power for each tissue element separately using the Bethe-Bloch equation, and then used Bragg's rule for compounds to determine the tissue's total stopping power. The total stopping power is directly proportional to the atomic number divided by the target material's atomic mass (Z/A) and target material density (ρ), and inversely proportional to the target material's mean excitation energy (I) and proton energy (E). The results indicate that the stopping power was highest in the adipose tissue, and the lowest value was in the bone (cortical) at the same proton energy. We performed all calculations using the MATLAB program. We found a good match between the obtained results and the value of the P-Star code.

Keywords: Total stopping power, proton energy loss, human tissue, Bethe-Bloch equation, Bragg's rule.

1. Introduction

The study of radiation energy loss in the material is one of the most important subjects in medical physics because of its multiple applications in radiation therapy. Furthermore, understanding the behavior of radiation in a material and its interactions plays a crucial role in determining the radiation dose during medical testing or radiation therapy, assessing the impact of this dose on cells adjacent to the target cells, and understanding the potential damage to adjacent tissues. Furthermore, estimating the appropriate radiation dose or determining the amount of a safe radiation dose during testing, therapy, or exposure to natural or artificial radiation is very important to protect a person from the possible risks of such radiation exposure [1-4].

Radiation therapy commonly treats cancer, with protons being the preferred choice due to their ability to regulate the radiation dose, concentrating the dose density in the affected area while exposing the surrounding area to minimal radiation [1,2]. Protons have properties that make them more efficient in radiation therapy than classical radiation since when protons enter the material, they lose a small amount of energy on the surface of the material, while the

maximum amount of energy loss occurs at the end of the path in the region called the Bragg Peak [3,4].This study aims to calculate the total stopping power of protons in some tissues of the body using the Bethe-Bloch equation for elements and Bragg's rule for compounds, and compare the results with P-Star results.

Many researchers have studied proton energy loss within human tissue and the stopping power of protons. Ahmed, I., Nowrin, H., and Dhar, H. (2020) conducted a study on the stopping power and range of protons in biological human soft and hard tissues, including blood, brain, skeleton-cortical bone, and skin, at energies ranging from 1 MeV to 350 MeV. They utilized the Bethe-Bloch formula and compared their findings with the SRIM program [5]. El-Ghossain, M. O., (2021) conducted a study on the interaction of protons with water and human body parts, calculating the energy loss, stopping power, and proton range for water, skin, bone, and adipose tissue within the energy range of 10 keV to 1000 MeV using the Bethe-Bloch formula, P-Star, and MATLAB [6]. Almutairi, A. S., and Osman, K. T. (2022) conducted a study on the mass stopping power, range, and important radiation quantities of protons in various biological human body parts, including water, muscle, skeletal, and cortical bone, within the energy range of 0.04 to 200 MeV, using the Bethe-Bloch formula and MATLAB program. Upon comparing the results with the data from P-STAR, they were found to be well-matched [7].

2. Methods and Material

2.1 Interaction of Nuclear Radiation with Material

The study of the interaction of nuclear radiation with materials is one of the fundamental subjects in radiation dose measurement, nuclear detector building, and other medical and industrial applications. Depending on the type of reaction and the amount of energy lost in the material with which the radiation interacts, two types of nuclear radiation exist: ionizing radiation and non-ionizing radiation [8,9].

There is another classification of nuclear radiation that depends on the type of radiation: first, charged particle radiation, which includes heavy charged particles (such as protons, deuterons, and alpha particles) and light charged particles (such as electrons), and secondly, uncharged particle radiation, which includes neutrons and electromagnetic rays (X-rays and Gamma Rays) [10,11].

2.2 Interaction of Heavy-Charged Particles

When heavy charged particles traverse a medium, they primarily interact with the medium's electrons due to the influence of Coulomb forces on both charged particles and electrons. Given the small size of the nucleus compared to the atom, the likelihood of heavily charged particles colliding with electrons is significantly higher than that of colliding with the nucleus. Therefore, the dominant mechanism for the loss of energy of charged particles is coulomb scattering by the electrons of atoms, which leads to excitation or ionization of the atom [12]. Heavy-charged particles can produce a large number of vertical and non-vertical collisions before they lose their entire energy, and since the range of Coulomb forces is infinite, these particles interact with a large number of electrons at the same time, so they will gradually lose their energy along their path until they stop moving and their path is almost in the form of a straight line [13].

2.3 Energy Loss of Proton in Material

There are many mechanisms by which a proton interacts with an atom or nucleus in the target material. Protons may have Coulombic interactions with atomic electrons, Coulombic

interactions with a nucleus, nuclear interactions, or the release of bremsstrahlung. A proton undergoes a set of these interactions through its path in material [14,15]. Table 1 shows possible proton interactions within the material.

Protons lose their kinetic energy due to inelastic Coulomb interactions, which include numerous inelastic collisions with atomic electrons, and elastic Coulomb interactions, which include collisions with the nucleus. Additionally, inelastic collisions between a proton and a nucleus may occur, although these collisions are unlikely. Moreover, protons can engage in an inelastic nuclear reaction with the nucleus, where the nucleus absorbs the proton and potentially releases the neutron. Nuclear interaction removes these protons, leading to a rapid decrease in their number at the end of the path. As for the release of deceleration photons, it is theoretically possible to release deceleration photons, but the probability of their occurrence is almost nil at high energies [16].

Most protons move in an almost straight line because their rest mass is equal to 938 MeV, which is about 1832 times greater than the electron's rest mass of 0.511 MeV. Repulsion forces deflect a proton near the nucleus, causing it to lose a small amount of energy in this type of scattering and causing a slight change in its path [17-19].

Table 1. Proton interactions within material [16].

Type of Interaction	Principal Ejectives	Interaction Target	Influence on Projectile
Inelastic Coulomb scattering	Primary proton, ionization electrons	Atomic electrons	Quasi-continuous energy loss
Elastic Coulomb scattering	Primary proton, recoil nucleus	Atomic nucleus	Change in trajectory
Non-elastic nuclear reactions	Secondary protons and heavier ions, neutrons, and gamma rays	Atomic nucleus	Removal of a primary proton from beam
Bremsstrahlung	Primary proton, Bremsstrahlung photon	Atomic nucleus	Energy loss, change in trajectory

3. The Theoretical Calculations

3.1 Stopping Power of Heavy Charged Particles

The stopping power of heavy charged particles represents the amount of energy that these particles lose per path unit in the material, and it does not depend on the mass of the charged particle but depends on the square of the atomic number of the charged particle, the speed of the charged particle in the material, and the density of material through which the charged particle passes [20,21].

The calculation of the energy loss of heavy-charged particles is carried out in practice by calculating the number of ion pairs generated during the path of the charged particle. If the amount of energy that a charged particle loses when generating one ion pair is equal to *w*, then the number of ion pairs per length unit of the charged particle's path is given by - $\frac{dE}{dx} = w_i$ Where *i* is the number of ionic pairs [22].

The energy loss in the material has been calculated theoretically by many researchers, but the classical derivation was by Bethe, who developed a mathematical formula for calculating the energy loss in the material. Bloch has improved this formula, which represents the stopping power of a charged particle in a material. The full formula of this equation can be expressed as follows [6,20]:

$$-\frac{dE}{dx} = \left(\frac{e^2}{4\pi\epsilon_o}\right)^2 \left(\frac{4\pi N_A z^2 Z\rho}{m_e c^2 \beta^2 A}\right)\left[ln\left(\frac{2m_e c^2\beta^2}{I}\right) - ln(1-\beta^2) - \beta^2\right] \quad (1)$$

Since the classical electron radius (r_e) is given by the following formula:

$$r_e = \frac{e^2}{4\pi\epsilon_o m_e c^2} = 2.818 \times 10^{-13} \text{ cm} \quad (2)$$

When reformulating Equation (1) using the classical electron radius, we get the following formula:

$$-\frac{dE}{\rho\, dx} = (4\pi N_A r_e{}^2\, m_e c^2)\left(\frac{z^2}{\beta^2}\right)\left(\frac{Z}{A}\right)\left[ln\left(\frac{2m_e c^2\beta^2}{I}\right) - ln(1-\beta^2) - \beta^2\right] \quad (3)$$

A negative signal indicates that the particle's energy decreases as its range in the material increases.

Where: $\frac{dE}{dx}$ stopping power, ρ density of material, $\frac{dE}{\rho\, dx}$ mass stopping power, N_A Avogadro number ($6.022\times10^{23}\ mol^{-1}$), m_e electron mass, c speed of light in vacuum, $m_e c^2$ rest energy for the electrons (0.511 MeV), z atomic number of the incident particle, Z atomic number of material, A atomic mass of material, I mean excitation energy, β is the rate between the speed of the particle and the speed of light in a vacuum. Since $(4\pi N_A r_e{}^2\, m_e c^2)$ = $(0.307075\ mol^{-1}\ cm^2)$ then:

$$-\frac{dE}{\rho\, dx} = 0.307075\left(\frac{z^2}{\beta^2}\right)\left(\frac{Z}{A}\right)\left[\ln\left(\frac{1.022\times10^6\,\beta^2}{I}\right) - ln(1-\beta^2) - \beta^2\right] \quad (4)$$

When calculating the total stopping power of heavy charged particles, the density correction resulting from the blocking of remote electrons by near electrons should be taken into account, which will reduce the energy loss of the charged particle at high energies, and the shell correction, which is important only at low energies, where the particle velocity is approximately equal to the orbital electron velocity [23,24].

It is important to note that the energy loss of the incident particle is inversely proportional to the square of the particle's velocity and directly proportional to the square of its charge and that the energy loss does not depend on the mass of the charged particle, but depends on the properties of the target material, which are density, atomic number, atomic mass, and mean excitation energy [25,26].

Table 2. Atomic number, atomic mass and mean excitation energy of the elements involved in the composition of the human tissue [27].

Element	**Z**	**A (mol^{-1})**	**Z / A**	**I (*e.V*)**
Hydrogen	1	1.0079	0.99216	19.2
Carbon	6	12.011	0.49955	78
Nitrogen	7	14.007	0.49976	82
Oxygen	8	15.999	0.50002	95
Sodium	11	22.99	0.47848	149
Magnesium	12	24.305	0.49373	156
Silicon	14	28.086	0.49848	173
Phosphorus	15	30.974	0.48428	173
Sulfur	16	32.065	0.49899	180
Chlorine	17	35.453	0.47951	174
Potassium	19	39.098	0.48595	190
Calcium	20	40.078	0.49903	191
Iron	26	55.845	0.46557	286
Zinc	30	65.39	0.45879	330

3.2 The Total Stopping Power of Protons in Human Tissue

When calculating the total stopping power of protons in the human tissue, human tissue is treated as a compound, composed of thin layers of pure elements included in the composition of that compound, and the energy of chemical bonds between the constituent elements is neglected, so the stopping power of the compound is equal to the sum of the total stopping power in each element, taking into account the percentage of participation of each element in that compound, and according to Bragg's rule for compounds, that is, the total stopping power in the compound material is written by the following formula [28-30]:

$$\left(\frac{S}{\rho}\right)_{comp} = \sum_i w_i \left(\frac{S}{\rho}\right)_i \quad (5)$$

$\left(\frac{S}{\rho}\right)_{comp}$ is the stopping power of the compound and w_i is the percentage weight of each element in the compound, which is calculated by the percentage weight ratios rule of the elements included in the chemical compounds, which is equal to the molar mass of the element in the number of atoms of the element on the molar mass of the compound and $\left(\frac{S}{\rho}\right)_i$ is the stopping power of each of the constituent elements of this compound.

Table 3. The weight percentages of the elements contained in the structure of the human tissues [31].

Element	Adipose tissue	Blood	Bone, Compact	Bone, Cortical	Brain	Eye lens	Lung	Skin	Testicles
Hydrogen	11.95	10.19	6.398	4.723	11.07	9.927	10.13	10.06	10.42
Carbon	63.72	10.00	27.8	14.43	12.54	19.37	10.23	22.83	9.227
Nitrogen	0.797	2.964	2.7	4.199	1.328	5.327	2.865	4.642	1.994
Oxygen	23.23	75.94	41.00	44.61	73.77	65.38	75.71	61.9	77.39
Sodium	0.05	0.185	0	0	0.184	0	0.184	0.007	0.226
Magnesium	0.002	0.004	0.2	0.22	0.015	0	0.073	0.006	0.011
Silicon	0	0.003	0	0	0	0	0	0	0
Phosphorus	0.016	0.035	7	10.50	0.354	0	0.08	0.033	0.125
Sulfur	0.073	0.185	0.2	0.315	0.177	0	0.225	0.159	0.146
Chlorine	0.119	0.278	0	0	0.236	0	0.266	0.267	0.244
Potassium	0.032	0.163	0	0	0.31	0	0.194	0.085	0.208
Calcium	0.002	0.006	14.7	20.99	0.009	0	0.009	0.015	0.01
Iron	0.002	0.046	0	0	0.005	0	0.037	0.001	0.002
Zinc	0.002	0.001	0	0.01	0.001	0	0.001	0.001	0.002

4. Results and Discussion

The Bethe-Bloch equation was used to calculate the total stopping power of protons in human tissue (Adipose tissue, Blood, Bone (Compact), Bone (Cortical), Brain, Eye lens, Lung, Skin and Testicles) in the energy range from 1 MeV to 1000 MeV. The total stopping power of the constituent elements of these tissues was calculated (Hydrogen, Carbon, Nitrogen, Oxygen, Sodium, Magnesium, Silicon, Phosphorus, Sulfur, Chlorine, Potassium, Calcium, Iron, Zinc), and then Bragg's rule for compounds was applied to calculate the total stopping power of the tissue, where the total stopping power of these elements was collected after multiplying it by the percentage of their participation in each tissue to find the total stopping power of each tissue separately. The total stopping power of the elements (Hydrogen, Carbon, Nitrogen, Oxygen,

Silicon, and Iron) was compared with the values of the universal code P-Star and it was found that the largest error rate was about 6% for Carbon, 4.5% for Nitrogen, 4.4% for Oxygen and 3.8% for Silicon and Iron, while the error rate of Hydrogen was less than 0.1%, as shown in Tables 4 and 5. As for the rest of the elements, they were not compared due to the unavailability of their data in the P-Star.

The total stopping power of (Adipose Tissue, Bone (Compact), and Bone (Cortical)) was also compared with the values of the universal code P-Star, and the largest error rate was about 4.8% for Adipose Tissue, 6% for Bone (Compact) and 6.4% for Bone (Cortical), as shown in Table 6. As for the rest of the tissues, they were not compared due to the unavailability of their data in the P-Star. Protons with energy that is less than 20 MeV lose a large amount of energy when they pass through the tissues compared to protons with greater energy (more than 20 MeV), because protons with large energy are fast and therefore will spend a short period inside the material and thus less likely to interact with the electrons and the nucleus, and thus the amount of energy lost decreases. It is noted that protons with large energy lose almost the same amount of energy, regardless of the target tissue, as shown in **Table 7**. From the obtained results, we notice that the protons behave the same in all the tissues studied and that the behavior of the protons is the same if the target material is an element or a compound, as shown in **Figure 1–Figure 4**. This process of proton energy loss in the material depends on the proton's properties (its energy and atomic number) and the target material's properties (its atomic number, mass, and mean excitation energy). This means that the proton's behavior in the material changes as its properties and the target material's properties change. However, the proton's behavior in the material stays the same whether it is an element or a compound as long as these properties stay the same.

Although the results do not exactly match the values of the Universal P-Star Code, the largest error rate was about 6%, which is considered an acceptable percentage; therefore, the Bethe-Bloch equation without corrections is considered an effective equation for calculating the total stopping power of the proton. We must add density correction and shell correction to the mentioned equation to obtain results that are completely identical to the P-Star values.

Table 4. Total stopping power ($MeV.cm^2.g^{-1}$) for Hydrogen, Carbon, and Nitrogen compared with the value of the universal code P-Star [27].

Proton Energy	Hydrogen			Carbon			Nitrogen		
	P-Star	This Work	Error %	P-Star	This Work	Error %	P-Star	This Work	Error %
1	677.1	677.12	0	226.3	239.88	6	226.1	236.38	4.5
2	388.5	388.68	0	139.5	145.1	4	138.9	143.35	3.2
4	219.7	219.77	0	83.3	85.27	2.4	82.91	84.4	1.8
6	156.7	156.66	0	60.84	61.9	1.7	60.6	61.32	1.2
8	123	123.02	0	48.47	49.17	1.4	48.31	48.73	0.9
10	101.9	101.92	0	40.57	41.07	1.2	40.44	40.72	0.7
20	56.79	56.77	0	23.18	23.38	0.8	23.13	23.2	0.3
40	31.82	31.8	0.1	13.24	13.33	0.7	13.22	13.24	0.1
60	22.85	22.84	0	9.6	9.66	0.6	9.59	9.59	0.1
80	18.18	18.17	0	7.68	7.73	0.6	7.67	7.68	0.1
100	15.3	15.3	0	6.49	6.53	0.6	6.49	6.49	0
200	9.33	9.32	0	4	4.02	0.7	4	4	0
400	6.24	6.24	0	2.69	2.72	1.1	2.7	2.7	0
600	5.23	5.23	0	2.26	2.29	1.5	2.28	2.28	0
800	4.76	4.76	0	2.05	2.09	2	2.08	2.08	0
1000	4.5	4.5	0	1.94	1.98	2.4	1.97	1.97	0

Table 5. Total stopping power (MeV.cm^2.g^{-1}) for Oxygen, Silicon and Iron compared with the value of the universal code P-Star [27].

Proton Energy	Oxygen			Silicon			Iron		
	P-Star	This Work	Error %	P-Star	This Work	Error %	P-Star	This Work	Error %
1	216.3	225.89	4.4	175.4	182.08	3.8	131.3	136.29	3.8
2	133.5	138.11	3.5	111.8	116.1	3.8	86.58	91.52	5.7
4	80.11	81.78	2.1	68.6	70.7	3.1	54.82	57.55	5
6	58.75	59.57	1.4	50.91	52.14	2.4	41.33	43.03	4.1
8	46.93	47.42	1	41.01	41.82	2	33.62	34.79	3.5
10	39.34	39.66	0.8	34.59	35.17	1.7	28.56	29.42	3
20	22.58	22.67	0.4	20.2	20.37	0.9	16.97	17.29	1.9
40	12.94	12.96	0.2	11.73	11.78	0.4	9.99	10.1	1.1
60	9.4	9.4	0.1	8.56	8.59	0.3	7.35	7.41	0.8
80	7.53	7.53	0.1	6.89	6.9	0.2	5.93	5.97	0.6
100	6.37	6.37	0	5.84	5.85	0.2	5.04	5.07	0.6
200	3.93	3.93	0	3.63	3.64	0.2	3.15	3.17	0.6
400	2.66	2.66	0	2.46	2.47	0.4	2.15	2.17	0.9
600	2.24	2.24	0	2.08	2.09	0.6	1.81	1.84	1.4
800	2.05	2.05	0	1.9	1.91	0.8	1.66	1.69	1.7
1000	1.95	1.95	0	1.8	1.82	1	1.57	1.61	2

Table 6. Total stopping power (MeV.cm^2.g^{-1}) for Adipose tissue, Bone (Compact) and Bone (Cortical) compared with the value of the universal code P-Star [27].

Proton Energy	Adipose tissue			Bone, Compact			Bone, Cortical		
	P-Star	This Work	Error %	P-Star	This Work	Error %	P-Star	This Work	Error %
1	275.5	288.66	4.8	233.9	247.88	6	219.6	233.63	6.4
2	166.8	172.47	3.4	143.6	150.63	4.9	135.5	143.05	5.6
4	98.35	100.48	2.2	85.76	88.81	3.6	81.42	84.79	4.1
6	71.46	72.64	1.7	62.76	64.57	2.9	59.76	61.79	3.4
8	56.77	57.55	1.4	50.08	51.33	2.5	47.77	49.2	3
10	47.41	47.99	1.2	41.96	42.9	2.2	40.08	41.16	2.7
20	26.96	27.19	0.8	24.06	24.46	1.7	23.07	23.53	2
40	15.34	15.44	0.7	13.78	13.96	1.3	13.26	13.46	1.5
60	11.1	11.17	0.6	10.01	10.12	1.1	9.64	9.77	1.4
80	8.87	8.93	0.6	8.02	8.1	1.1	7.72	7.83	1.3
100	7.5	7.54	0.6	6.78	6.85	1.1	6.54	6.62	1.3
200	4.61	4.63	0.5	4.19	4.23	1	4.04	4.09	1.1
400	3.11	3.12	0.5	2.83	2.86	0.9	2.74	2.77	1
600	2.62	2.63	0.5	2.39	2.41	0.9	2.31	2.33	1
800	2.39	2.4	0.5	2.17	2.2	1.3	2.11	2.13	1.2
1000	2.26	2.27	0.8	2.05	2.09	1.7	1.99	2.02	1.6

Table 7. Total stopping power (MeV.cm^2.g^{-1}) for Protons in the human tissues.

Proton Energy	Adipose tissue	Blood	Bone, Compact	Bone, Cortical	Brain	Eye lens	Lung	Skin	Testicles
1	288.66	273.11	247.88	233.63	277.08	273.95	272.79	274.67	273.92
2	172.47	164.25	150.63	143.05	166.46	164.62	164.08	165.01	164.72
4	100.48	96.14	88.81	84.79	97.36	96.3	96.05	96.5	96.4
6	72.64	69.66	64.57	61.79	70.52	69.75	69.6	69.9	69.85
8	57.55	55.27	51.33	49.2	55.93	55.33	55.22	55.44	55.41
10	47.99	46.13	42.9	41.16	46.67	46.17	46.08	46.26	46.25
20	27.19	26.2	24.46	23.53	26.5	26.22	26.18	26.27	26.27
40	15.44	14.91	13.96	13.46	15.08	14.92	14.9	14.94	14.95
60	11.17	10.79	10.12	9.77	10.91	10.8	10.79	10.82	10.82
80	8.93	8.63	8.1	7.83	8.73	8.63	8.63	8.65	8.65
100	7.54	7.29	6.85	6.62	7.37	7.29	7.29	7.31	7.31
200	4.63	4.49	4.23	4.09	4.54	4.49	4.49	4.5	4.5
400	3.12	3.03	2.86	2.77	3.06	3.03	3.03	3.03	3.04
600	2.63	2.55	2.41	2.33	2.58	2.55	2.55	2.56	2.56
800	2.4	2.33	2.2	2.13	2.35	2.33	2.33	2.33	2.33
1000	2.27	2.21	2.09	2.02	2.23	2.21	2.21	2.21	2.21

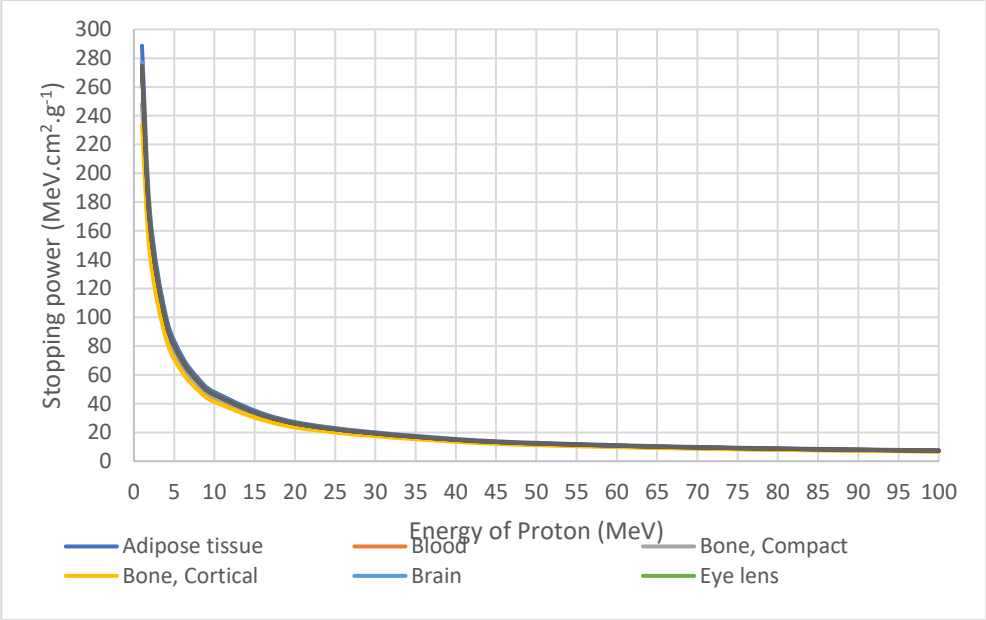

Figure 1. The stopping power of Proton in human tissue at the energy range from 1 to 100 MeV.

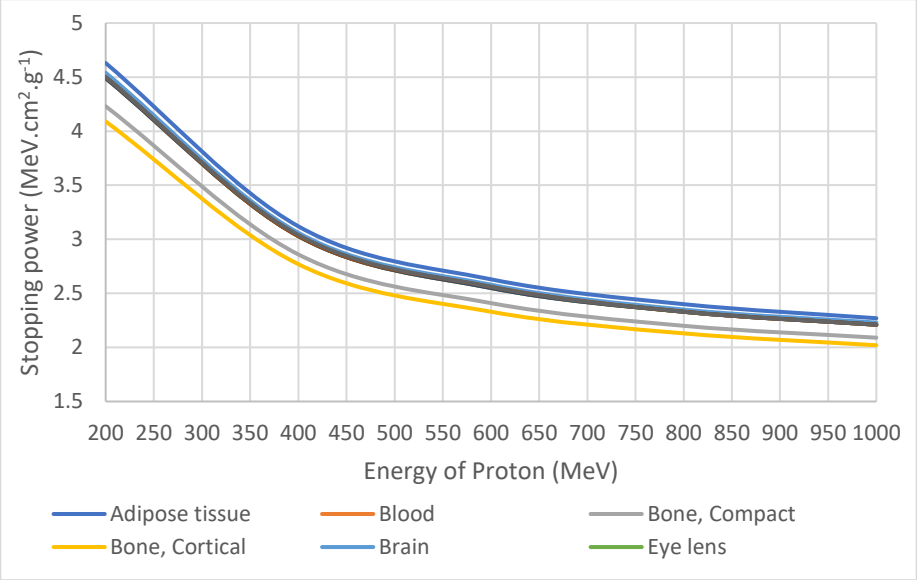

Figure 2. The stopping power of Proton in human tissue at the energy range from 200 to 1000 MeV.

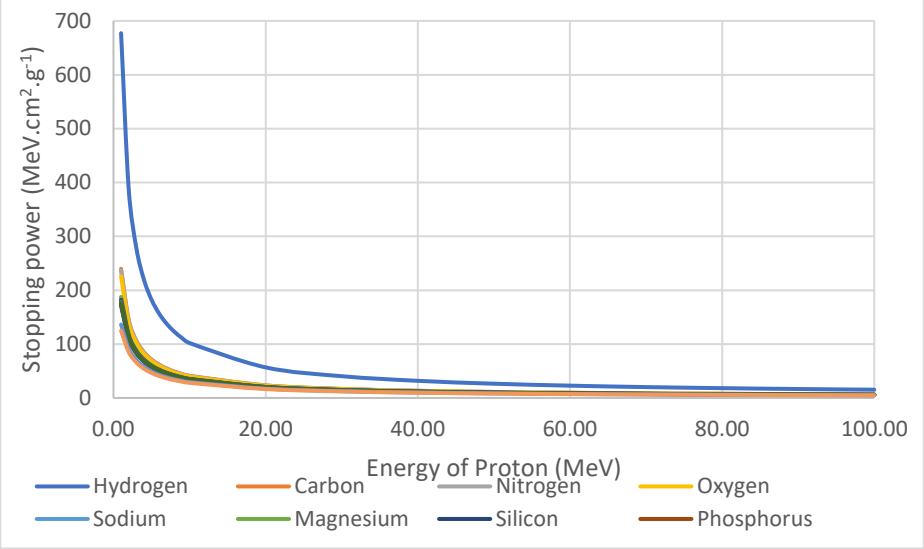

Figure 3. The stopping power of Proton in the constituent elements of human tissue at the energy range from 1 to 100 MeV.

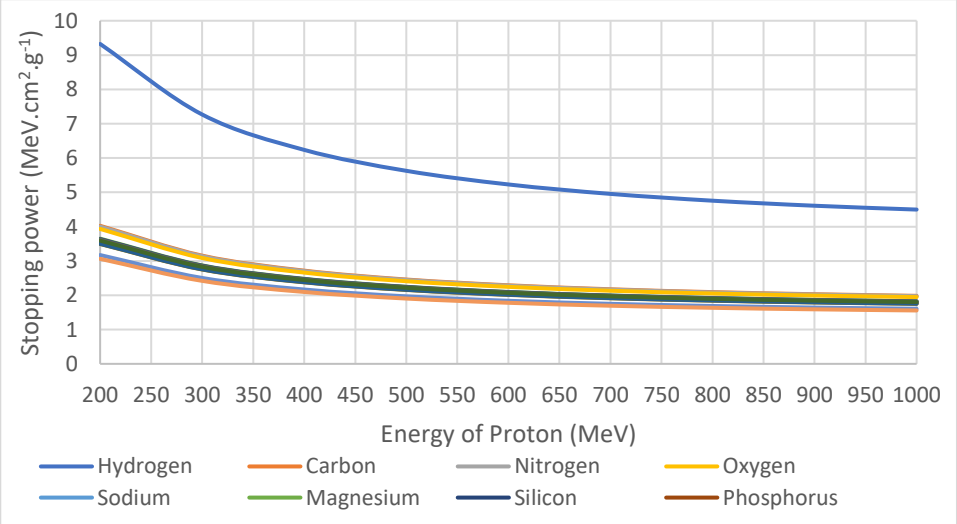

Figure 4. The stopping power of Proton in the constituent elements of human tissue at the energy range from 200 to 1000 MeV.

5. Conclusion

The stopping power depends on the energy of the incident proton and the target material's atomic number, atomic mass, and mean excitation energy. The stopping power decreases with increasing the incident proton energy, where the higher the proton's energy, the higher its speed, and therefore the amount of β increases, which equals $\frac{v}{c}$, and since the stopping power is inversely proportional to β, this leads to a decrease in stopping power.

The quantity $(\frac{Z}{A})$ decreases with increasing the atomic number, and the stopping power decreases with decreasing the quantity $(\frac{Z}{A})$. Therefore, the stopping power is inversely proportional to the atomic number Z of the target material.

The stopping power is inversely proportional to the mean excitation energy *I*, the smaller the value of the mean excitation energy, the greater the amount of energy lost and the probability of ionization of the atom, and therefore the stopping power increases.

The stopping power is directly proportional to the density of the target material, so the higher the density of the material, the greater the stopping power.

The greatest value of the total stopping power is at low energies, and it begins to decrease as the energy of the incident proton increases. The stopping power of a slow proton (low energy proton) is much greater than the stopping power of a fast Proton (high energy proton) because the slow proton spends a longer period in the atom, and therefore the probability of its interaction with electrons increases, leading to excitation or ionization of the atom.

The largest error rate was at low energies, and then the error rate began to decrease as the incident proton energy increased, and that is because of not adding shell correction to the equation used.

Acknowledgment

All thanks and appreciation to the College of Sciences, University of Tikrit for their valuable comments on this article, and thanks go to the journal's management and members.

Conflict of Interest

The authors declare that they have no conflicts of interest.

Funding

None**.**

Ethical Clearance

None.

References

1. Hussien, A.H. Stopping Power for Carbon, Oxygen and Proton Interacting with Adipose Tissue, Skeletal, Muscle and Brain Using Different Formulas. *European Journal of Mprimarycular & Clinical Medicine* **2020**, *7*, 494-503. https://doi:a7d098333ed6efecf625158e d f0cdd04
2. Hadi, S.M.; Bashair M.S. Theoretical Study for the Calculation of Proton Range in Human Body Tissues. *Iraqi Journal of Science* **2021**, *23*, 3392-3399. https://doi.org/10.24996/ijs.2021.62.9(SI).10

3. Bichsel, H.; Heinrich S. The interaction of radiation with matter. *Particle Physics Reference Library: Detectors for Particles and Radiation* **2020**, *2*, 5-44. https://doi.org/10.1007/978-3-030-35318-6_2
4. Semwal, M. Khan's the physics of radiation therapy. *Journal of Medical Physics* **2020**, *2*, 134-135. https://doi.org/10.4103%2Fjmp.JMP1720
5. Ahmed, I.; Hridita, N.; Hriday, D. Stopping power and range calculations of protons in human tissues. *Baghdad Science Journal* **2020**, *4*, 1223-1223. http://dx.doi.org/10.21123/bsj.2020.17.4.1223
6. El-Ghossain, M.O. Proton Interaction with Water and Human Body Parts Calculations of Range and Stopping Power. *International Journal of Applied Physics* **2021**, *8*, 32-35. https://doi.org/10.14445/23500301/IJAP-V8I1P105
7. Almutairi, A.S.; Khalda, T.O. Calculation of Mass Stopping Power and Range of Protons as Well as Important Radiation Quantities in Some Biological Human Body parts (Water, Muscle, Skeletal and Bone, Cortical). *International Journal of Medical Physics* **2022**, *2*, 99-112. https://doi.org/10.4236/ijmpcero.2022.112009
8. El-Ghossain, M.O. Calculations of stopping power, and range of electrons interaction with different material and human body parts. *Int J Sci Technol Res* **2017**, 6(*1*), 114-8. https://core.ac.uk/download/ pdf/287990709.pdf
9. Yaqoob, S.N.; Bashair, M.S. Calculation of Stopping Power and Range of Nitrogen Ions with the Skin Tissue in the Energies of (1-1000) MeV. *Ibn AL-Haitham Journal for Pure and Applied Sciences* **2018**, *2*, 69-78. https://doi.org/10.30526/31.2.1945
10. Hadi, H.S.; Rashid, O.K. Stopping Power Calculations of Electron in Six Types of Human Tissue for Energies (20-20000eV). *Journal of Kufa-Physics* 2017, *1*, 23-35. https://doi:index.php/jkp/article/view/7340
11. Mayles, P.; Nahum, A.E.; Rosenwald, J.C. Handbook of Radiotherapy Physics: Theory and Practice. *Taylor & Francis Group* **2021**, *2*, 243-255. https://doi.org/10.1201/9780429201493
12. El-Ghossain, M.O. Calculations of stopping power, and range of ions radiation (alpha particles) interaction with different materials and human body parts. *Int. J. Phys.* **2017**, *3*, 92-98. https://doi:12.232/ijp/5/3/5/index.html
13. Osman, H.; Hasan, G. Stopping power and CSDA range calculations of electrons and positrons over the 20 eV–1 GeV energy range in some water equivalent polymer gel dosimeters. *Applied Radiation and Isotopes* **2022**, *179*. https://doi.org/10.1016/j.apradiso.2021.110024
14. Almutairi, A.S.; Khalda, T.O. Mass Stopping Power and Range of Protons in Biological Human Body Tissues (Ovary, Lung and Breast). *International Journal of Medical Physics, Clinical Engineering and Radiation Oncology* **2021**, *1*, 48-59. https://doi.org/10.4236/ijmpcero.2022.111005
15. Gottschalk, B. Radiotherapy proton interactions in matter. *preprint arXiv* **2018**, *12(3)*, 45-55. https://doi:arxiv.org/pdf/1804.00022
16. Newhauser, W.D.; Rui, Z. The physics of proton therapy. *Physics in Medicine & Biology* **2015**, *8*, 112-134. https://doi.org/article/10.1088/0031-9155/60/8/R155
17. Lechner, A. CERN: Particle interactions with matter. *CERN Yellow Rep. School Proc*. **2018**, *5*, 47. https://doi.org/10.23730/CYRSP-2018-005.47
18. Tandon, P. Interaction of ionizing radiation with matter. Radiation Safety Guide for Nuclear Medicine Professionals. *Singapore: Springer Nature Singapore* **2022**, *12*, 21-35. https://doi.org/10.1007/ 978-981-19-4518-23
19. Sharon, M.; Madhuri, S. Interaction of Radiation with Matter. Nuclear Chemistry. *Cham: Springer International Publishing* **2021**, *33*, 45-51. https://doi.org/10.1007/978-3-030-62018-9_4

20. Kadhim, R.O.; Razzag, D.F. Calculation of Protons Stopping Power in Some Organic Compounds for Energies (0.02-1000) MeV. *International Journal of Science and Research* **2013**, *4*, 2391-2393. https://doi:archive/v4i6/SUB155828.112
21. Alshibel, A.; Khalda, T.O. Mass Stopping Power and Range of Alpha Particles in Biological Human Body Tissues (Blood, Brain, Adipose and Bone). *Library Journal* **2023,** *10*, 1-17. https://doi.org/10.4236/oalib.1110775
22. Quashie, E.; Alfredo A.C. Electronic stopping power of protons and alpha particles in nickel. *Physical Review B* **2018**, *98*, 23. https://doi.org/10.1103/PhysRevB.98.235122
23. Zeman, E.M.; Eric C.S.; Joel, E.T. Basics of radiation therapy. *Abeloff's clinical oncology*. *Elsevier* **2020**, *34*, 431-460. https://doi.org/10.1016/B978-0-323-47674-4.00027-X
24. Katsumura, Y.; Hisaaki K. Interactions Between Radiation and Matter. *Radiation Applications* **2018**, *45*, 7-14. https://doi.org/10.1007/978-981-10-7350-22
25. Abd, S.A.; Kadhim, R.O. Calculation of Stopping Power for protons in Biological Human parts. *La Prensa Medica Argentina* **2020**, *106*, 1-4. https://doi.org/10.47275/0032-745X-245
26. Giri, K.; Rupa K. Energy loss of proton beam on ovary tumor. *Journal of Nepal Physical Society* **2019**, *1*, 24-29. https://doi.org/10.3126/jnphyssoc.v5i1.26879
27. Berger, M.J.; Coursey, J.S.; Zucker, M.A.; Chang, J. Stopping power and range tables for electrons, protons, and helium ions, NIST Standard Reference Database 124. *National Institute of Standards and Technology (NIST), Physical Measurement Laboratory (PML)* **2017**, *12*, 34-46 https://doi:11254.56/Star/Text/PSTAR.html
28. Hadi, S.M.; Bashair M.S. Stopping power and range of proton interaction with Al2O3, ZrO2 and SiO2. *AIP Conference Proceedings* **2019**, *1*, 23-36. https://doi.org/10.1063/1.5141441
29. Van Abbema, J.K. High accuracy proton relative stopping power measurement. *Nuclear Instruments and Methods in Physics Research Section B: Beam Interactions with Materials and Atoms* **2018**, *436*, 99-106. https://doi.org/10.1016/j.nimb.2018.09.015
30. Jassim, M.K. A Comparative Study for the Proton Electronic Stopping Power of Some Polymers by Using Mathematica, SRIM2013, PSTAR, LibdEdx, and Experimental Databases. *Ibn AL-Haitham Journal for Pure and Applied Sciences* **2017**, *2*, 43-53. https://doi.edu.iq/index.php/j/article/view/1453/1209
31. Detwiler, R.S. Compendium of material composition data for radiation transport modeling. No. PNNL-15870-Revision-2. *Pacific Northwest National Lab. (PNNL), Richland, WA (United States)* **2021**, *23*, 55-67. https://www.osti.gov/biblio/1782721